Int. J. Multiphase Flow Vol. 15, No. 4, pp. 483–493, 1989
Printed in Great Britain

0301-9322/89 $3.00 + 0.00
Maxwell Pergamon Macmillan/Elsevier

EXPERIMENTS ON VOID FRACTION WAVES

J. M. SAIZ-JABARDO† and J. A. BOURÉ
Commissariat à l'Energie Atomique, Service d'Etudes Thermohydrauliques, Centre d'Etudes Nucléaires de Grenoble, 85X, 38041 Grenoble Cedex, France

(*Received* 11 *May* 1988; *in revised form* 12 *December* 1988)

Abstract—Experiments on the propagation of small void fraction disturbances along an upward vertical test section are reported, for bubbly flows and transitional (bubbly–slug) flows. Wave attenuation and propagation speeds are discussed. In particular, it is shown that two propagation phenomena, with different speeds, may coexist, the higher speed wave being closely correlated with the appearance of slugs.

Key Words: void fraction, waves, slug, bubble, transition, two-phase flow

1. INTRODUCTION

Propagation phenomena play a major part in two-phase flow behavior. For void fraction disturbances, the concept of kinematic waves was first applied to two-phase flows by Wallis and Zuber (Zuber & Hench 1962; Zuber & Findlay 1965; Wallis 1969), in relation with two-phase flow modeling. Several research works have been devoted recently to the propagation of void fraction waves. Mercadier (1981) has examined the propagation of natural and induced void fraction waves in an annular vertical test section, for liquid superficial velocities in the range 0–1.5 m/s. Later on, Micaelli (1982) conducted experiments in a vertical test section of square cross section, for high superficial velocities of the liquid (1–10 m/s). Bernier (1982), working with a pipe of circular cross section, for low liquid superficial velocities (0–0.32 m/s), observed the propagation of naturally occurring void fraction waves. So did Matuszkiewicz *et al.* (1987) for superficial velocities of the liquid of the order of 0.2 m/s. Lately, Pauchon & Banerjee (1986) and Kytömaa (1986) have studied naturally occurring void fraction waves in circular test sections, while Tournaire (1987) has considered induced waves (see also Bouré 1988). Most of the works have adopted impedance voidmeters, flush mounted on the pipe wall. The work by Pauchon & Banerjee (1986) is the exception, since they adopted a γ-densitometer. Most of the works have studied a range of void fractions up to 0.2. Matuszkiewicz *et al.* (1987) and Tournaire (1987) have gone further, up to void fractions of the order of 0.5 and 0.4, respectively. As a result, they were able to investigate the transition between bubbly and slug flow regimes, and its relation with void fraction waves.

The work described here was primarily aimed at covering some gaps left by the foregoing investigations. Since the range of void fractions considered in this work was relatively large (up to 0.4), some transitional (bubbly–slug) effects have been observed. These effects have enabled us to propose an objective criterion for the transition. In addition, the combination of high-speed videotapes with the measurement of transient two-phase flow by impedance sensors distributed along the test section has allowed us to correlate the propagation speed of void fraction waves with the speed of displacement of Taylor bubbles in developed slug flow.

2. TEST SECTION AND OPERATING CONDITIONS

A schematic diagram of the loop is shown in figure 1. The test section (TS) was made out of Plexiglas in order to visualize the flow development. Its height was 2 m, and its cross section was circular of 25 mm i.d. Nitrogen instead of air was used as the gas phase given its availability. A set of six rotameters placed in parallel measured the gas flow rate, covering a range from 0 to 80 Nm^3/h. The water was circulated with a pump in a closed loop. In order to control the water temperature a heat exchanger was installed, using tap water as the cooling medium. Three parallel

†Present address: Escola Politécnica da Universidade de São Paulo, São Paulo, Brasil.

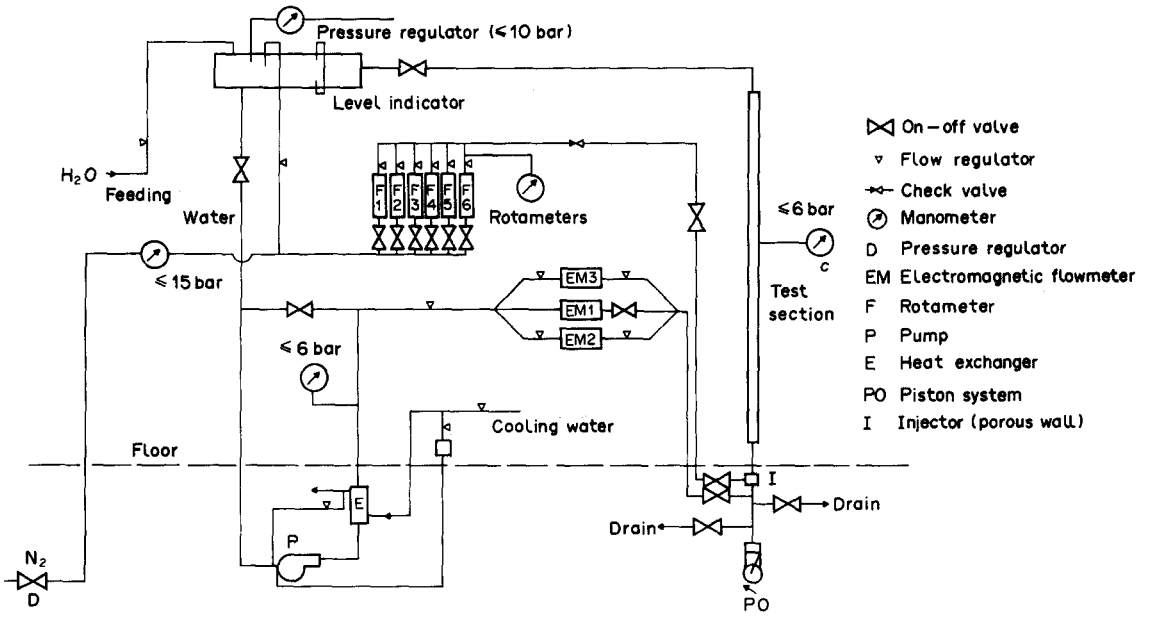

Figure. 1. Schematic diagram of the test loop.

electromagnetic flowmeters measured the water flow rate, covering the range 0–11.4 N m^3/h. The two-phase mixture at the exit of the test section was directed towards a pressurized tank, where a pressure regulator maintained the pressure in the test section. Induced perturbations of the void fraction were obtained through a piston system, shown schematically in figure 2. The amplitude of the perturbations could be adjusted by varying the course of the piston. The frequency could be changed by varying the motor speed.

Two types of impedance void fraction meters were used: with two and six electrodes (Tournaire 1987; Delhaye *et al.* 1987; Saiz-Jabardo 1987). Ten voidmeters with two electrodes (TES) were distributed along the TS, 20 cm apart from each other. Halfway between each TES pair, six-electrode voidmeters (SES) were installed, totalling nine of those sensors. The height of the voidmeters (2 cm) was established as a comparison between the necessity of measuring waves of sufficiently small wavelength, and the intent of reducing single-bubble effects. Edge effects were significantly reduced by guard rings, positioned as shown in figure 3, where the voidmeters are illustrated.

The operation mode of the voidmeters is resistive since a (low frequency) source signal of 20 kHz has been adopted. Variations of the resistance of the two-phase medium are "transformed" into voltage variations. The resultant signal is filtered, rectified and demodulated before being split into two different circuits: the first one extracts the average value of the signal through low-pass filtering, while the second provides the perturbations.

The voidmeters were calibrated by the gravimetric procedure (Delhaye *et al.* 1987; Saiz-Jabardo 1987), since the flow rates were low enough to make the friction effects negligibly small. One of the calibration curves is shown in figure 4, for a pressure of 4 b. Pressures of 3 and 4 b at the TS were adopted throughout the experiments in order to reduce the density variation effects. Liquid flow rates were generally low, corresponding to superficial velocities of 0, 0.120, 0.260 and 0.275 m/s. Given the low flow rates at which the loop was operated, the imposed frequencies of perturbation of the void fraction were limited to a maximum of 4 Hz. In addition, experiments without induced perturbations were also conducted, allowing us to compare results from both natural and induced perturbations. Finally, the adopted void fractions varied in the range 0.05–0.40. It was observed throughout the experiments that the void fraction along the TS presented only small variations even though there was a clear flow development between the lowermost position and the outlet of the TS. The effect of this flow development over the wave characteristics has been found to be negligibly small, except, of course, for those waves which are either strongly damped or amplified.

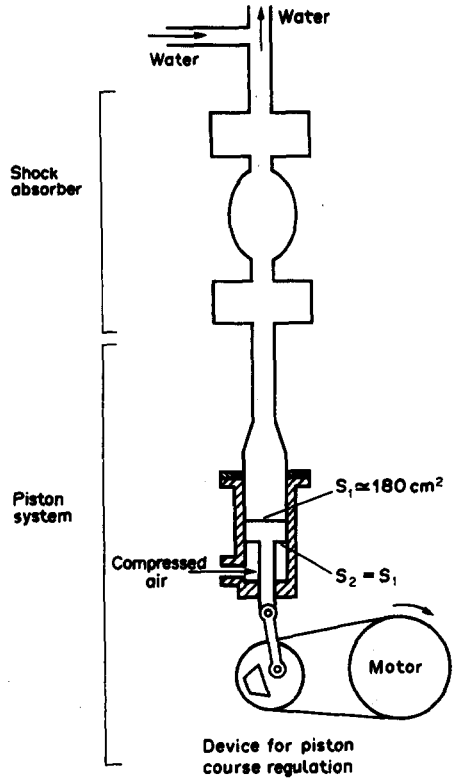

Figure 2. Piston perturbation system.

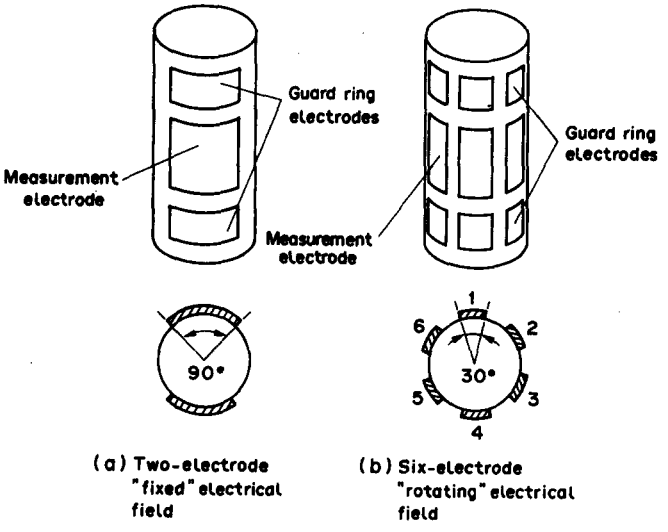

Figure 3. The two types of sensors used.

The electronically processed signal from the voidmeters was analyzed by a Plurimat *S* (Intertechnique, France) system. The joint analysis of two consecutive sensors provided the following parameters: γ^2_{xy} (coherence), $|H|$ (gain), ϕ (phase angle) and C_{xy} (cross-correlation). Also obtained was the spectrum of the signal from each voidmeter, which provides an accurate frequency measurement of the induced perturbations. The above parameters were relevant in determining

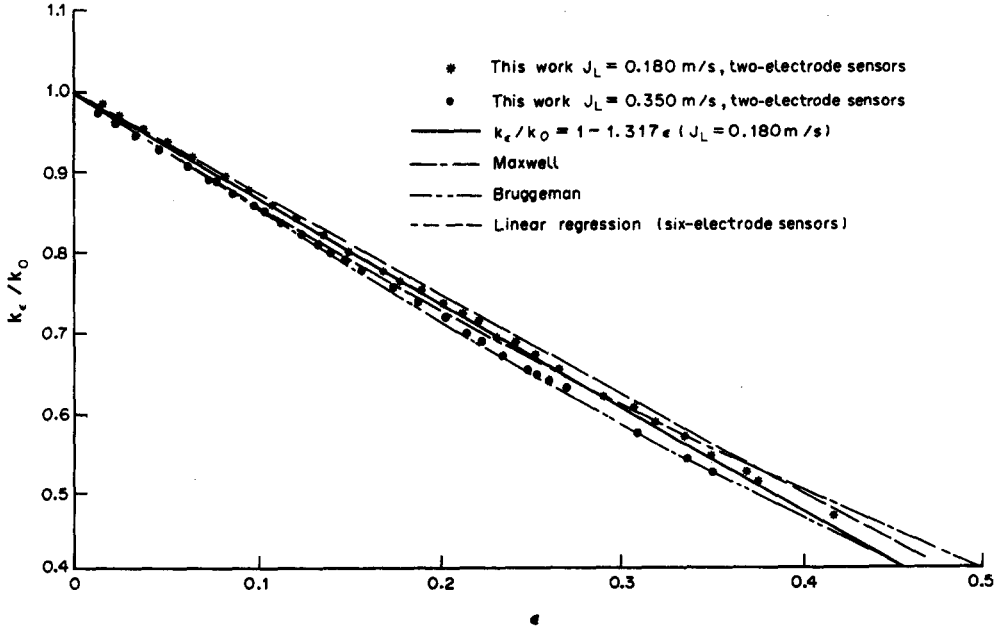

Figure 4. Calibration curve compared to other works.

such important aspects of the wave propagation as attenuation, through $|H|$,† and propagation speed, through either ϕ or C_{xy}.

3. RESULTS

In the analysis of wave propagation two parameters should be considered: (1) the wave attentuation characteristics of the propagation medium; and (2) the propagation speed. These aspects have been the main objective of the present study, and as such they will be discussed separately.

3.1. Wave attenuation

The attenuation of void fraction waves has been observed to be affected by both the frequency, and the mixture flow rate. These effects have been studied by previous researchers, and their general trends were confirmed by the present work, which, in addition, uncovered some relevant features of the problem. The observed results can be summarized as follows:

(a) Increments in the mixture flow rate reduce wave attenuation. This effect is easily confirmed when one compares results obtained by Micaelli (1982) with those from the present work. The former results were obtained for high values of J_L (>1 m/s). It was observed there that waves of 3 Hz were barely damped, and significant attentuation occurred only for frequencies >10 Hz. On the other hand, as figure 5 indicates, waves of frequency of the order of 3 Hz are significantly attentuated for $J_L = 0.275$ m/s. The same trend has been observed by Tournaire (1987). This effect is easily explained by the entrainment of the wave by the overall flow velocity: for a given time attenuation coefficient, the faster the wave, the smaller the apparent attenuation between two fixed sensors.

(b) Figure 5 also shows a strong effect of the frequency of the wave over the attenuation capacity of the two-phase medium. For the highest frequency (3.3 Hz) the wave is strongly damped as it moves along the TS. At the top, the wave has lost its identity. This does not happen at lower frequencies. Coherence values are intimately related with the attenuation effect. It has been observed that, as long as the wave is relatively strong, the coherence of signals of adjacent voidmeters presents values close to one. However, when the wave is strongly attenuated, losing its identity the coherence assumes values significantly lower than one, as can be seen in table 1, which displays values of coherence and propagation speed along the TS for the same conditions as figure 5.

(c) It has been observed that the strong attenuation which occurs for waves of higher frequencies is related to the formation of a bubble "structure" which moves at a higher speed than the original wave. In table 1 this effect can be clearly seen; and in table 2 also, which presents data for a higher void fraction than that in table 1.

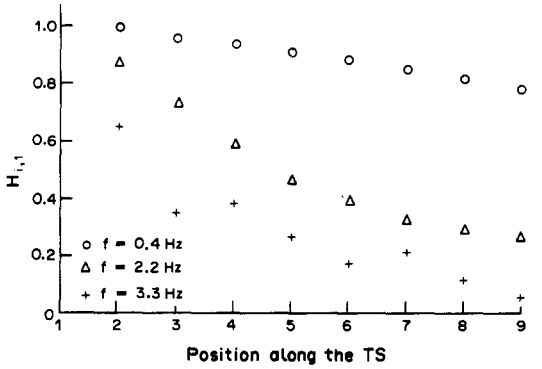

Figure 5. Gain along the TS with respect to the first sensor; $\epsilon = 0.053$, $J_L = 0.275$ m/s; $J_G = 0.025$ m/s.

†From now on $|H|$ will be noted H for simplicity.

Table 1. Coherence function and propagation speed ($\epsilon = 0.053$, $J_L = 0.275$ m/s, $J_G = 0.025$ m/s)

	$f = 0.4$ Hz		$f = 2.2$ Hz		$f = 3.3$ Hz	
Couple	γ^2_{xy}	c (m/s)	γ^2_{xy}	c (m/s)	γ^2_{xy}	c (m/s)
1–2	0.98	0.50	1.00	0.50	0.95	0.50
2–3	0.97	0.50	1.00	0.50	0.82	0.50
3–4	0.98	0.50	1.00	0.49	0.89	0.51
4–5	0.98	0.50	0.98	0.49	0.83	0.51
5–6	0.98	0.50	1.00	0.50	1.00	0.51
6–7	0.98	0.50	0.98	0.50	1.00	0.51
7–8	0.99	0.50	0.95	0.50	0.76	0.53
8–9	0.99	0.50	0.95	0.50	0.30	0.53

(d) Eventually, for void fractions about 0.10 (this is a rather arbitrary threshold), it has been observed that waves of high frequency are attenuated rapidly, originating a bubble "structure" which propagates at a higher speed than the original wave. It was also observed that both propagation speeds occur simultaneously along the TS. The orginal lower speed wave may eventually disappear at the top of the TS, the second rapidly moving structure prevailing. The appearance of the high speed is related, as mentioned before, to the complete attenuation of the original wave. Table 3, valid for $J_L = 0.260$ m/s and $\epsilon = 0.238$ illustrates this effect. This point will be further developed in section 4.

(e) In the range of void fractions characteristic of slug flow, it has been observed that there is a frequency range called the characteristic frequency range (CFR), such that a perturbation will be amplified if its frequency is in that range. On the other hand, if the frequency of the perturbation is outside the CFR (only the higher limit of the range has been tested), it will be attenuated. Figures 6(a–c) display results for $J_L = 0.275$ m/s and $\epsilon = 0.398$. Note that in figure 6(a) the 4.0 Hz wave is completely attenuated, while lower frequency waves are not. The spectrum of the above-mentioned 4.0 Hz perturbation is shown in figures 6(b, c) for measuring stations at the entrance and the exit of the TS, respectively. It can be seen therein that the original 4.0 Hz wave is strongly attenuated, in such a way that at the top it no longer exists [figure 6(c)]. On the other hand, frequency perturbations in the CFR (higher limit may be of the order of 3.0 Hz) are significantly amplified along the TS [refer to figures 6(b, c)]. Based on our own experiments and on other (França 1987; Jones & Zuber 1975), it can be concluded that the CFR is strongly dependent upon the mixture flow rate, as already discussed above in paragraph (a).

3.2. Propagation speed

Two methods have been used in this work to measure the propagation speed of the void fraction wave. One of them is based upon the phase angle, ϕ, of the cross-spectrum of the signals from two adjacent voidmeters. The other is based upon the well-known cross-correlation technique. Values obtained from each procedure were used to cross-check each other.

Table 2. Coherence function and propagation speed ($\epsilon = 0.105$, $J_L = 0.275$ m/s, $J_G = 0.055$ m/s)

	$f = 2.2$ Hz		$f = 3.1$ Hz		$f = 3.7$ Hz	
Couple	γ^2_{xy}	c (m/s)	γ^2_{xy}	c (m/s)	γ^2_{xy}	c (m/s)
1–2	0.98	0.47	0.93	0.47	0.89	0.47
2–3	0.97	0.47	0.94	0.47	0.89	0.47
3–4	0.96	0.47	0.94	0.48	0.38	0.48
4–5	0.96	0.47	0.60	0.48	0.33	0.48
5–6	0.96	0.47	0.55	0.48	0.24	0.49
6–7	0.99	0.47	0.54	0.49	0.20	0.50
7–8	0.98	0.47	0.27	0.49	0	0.51
8–9	0.92	0.47	0.31	0.50	0.12	0.53

Table 3. Coherence function and propagation speed ($\epsilon = 0.238$, $J_L = 0.260$ m/s, $J_G = 0.111$ m/s)

	$f = 2.8$ Hz		$f = 3.2$ Hz	
Couple	γ^2_{xy}	c (m/s)	γ^2_{xy}	c (m/s)
2–3	0.90	0.46	0.61	0.60
3–4	0.62	0.45	0.95	0.59
4–5	0.90	0.47	0.87	0.62
5–6	0.82	0.59	0.91	0.60
6–7	0.22	0.60	0.93	0.62
7–8	0.64	0.60	0.89	0.62
8–9	0.51	0.60	0.88	0.62

Results obtained by previous researchers have been confirmed by the present work, especially those of Mercadier (1981), Bernier (1982) and Tournaire (1987). Those works dealt with either natural (Mercadier 1981; Bernier 1982) or induced (Tournaire 1987) perturbations of void fraction. In this work both conditions have been examined, allowing us to observe an interesting behavior of the void fraction waves with respect to their propagation speeds. It has been observed that low-frequency induced perturbations propagate at the same speed as their natural counterparts. However, as the perturbation frequency is increased to the point of being severely damped along the TS, a second bubble "structure", may originate and two propagation speeds may eventually coexist. If the frequency is sufficiently high, as well as the void fraction, only the higher speed structure will occur at the top of the TS (resulting from the complete attenuation of the original

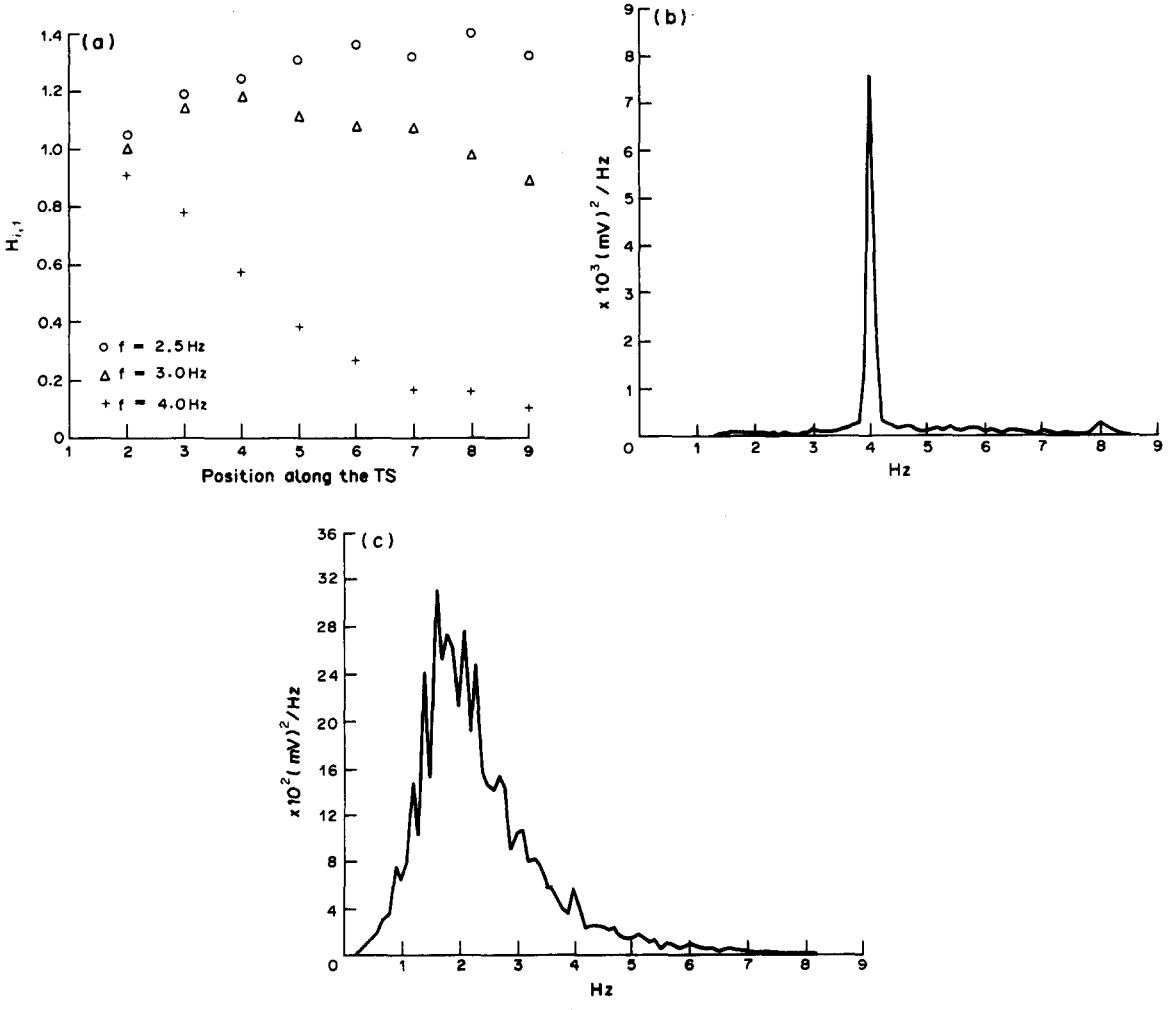

Figure 6. $\epsilon = 0.398$, $J_L = 0.275$ m/s, $J_G = 0.239$ m/s. (a) gain along the TS with respect to the first sensor; (b) spectrum at the bottom of the TS, $f = 4.0$ Hz; (c) spectrum at the top of the TS, $f = 4.0$ Hz.

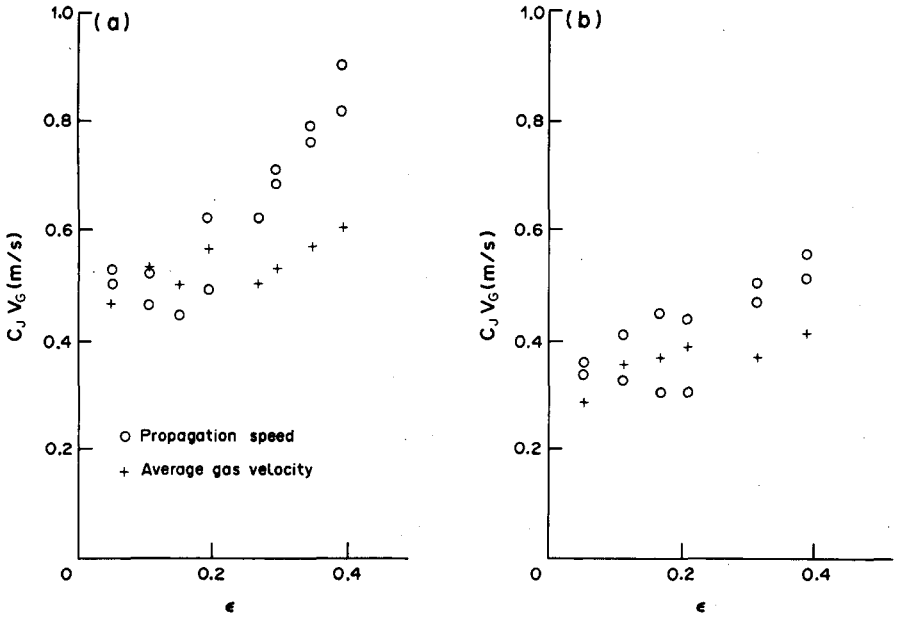

Figure 7. Propagation speeds at the top of the TS: (a) $J_L = 0.275$ m/s; (b) $J_L = 0.120$ m/s.

perturbation). Figures 7(a, b) show that behavior. In the figures, the average velocity of the gas phase is also plotted as a reference and the propagation speeds were obtained at the top of the TS. Note that two propagation speeds occur for all void fractions. The lower one corresponds to low-frequency natural perturbations, while the higher one is typical of the high-frequency perturbations, which were completely attenuated. Thus, the second propagation speed is characteristic of the newly born structure resulting from the attenuation of the original perturbation. It has also been observed that the higher propagation speed is higher than the average velocity of the gas phase.

With respect to previous works, figures 7(a, b) show a clear consistency. Regarding the low-frequency propagation speed, a slight decrease in the propagation speed can be observed up to void fractions of the order of 0.20, confirming results by Bernier (1982) and Mercadier (1981), who operated in this range of void fractions. Above this range, a steep increment in the propagation speed is observed. This behavior is certainly related to transitional effects.

The operation at relatively high void fractions has allowed us to observe transitional effects and even the developed slug flow regime. Signals obtained from the voidmeters for bubbly, transitional and slug flow regimes are shown in figures 8(a–c), respectively. In addition, high-speed videotapes of the flow allowed us to cross-check results obtained from the voidmeter signals. In table 4, the frequency of slugs obtained from the videotapes is compared to that from the spectrum of the signal from the voidmeters. A significant coincidence can be observed. For a void fraction of 0.398, and $J_L = 0.275$ m/s, when slug flow regime has been established, the observed frequency of the slugs was 3.4 Hz, for a case where there was no imposed perturbations (NP). The case where the frequency of the imposed perturbation is outside the CFR is also shown in table 4 for $\epsilon = 0.398$, $J_L = 0.275$ m/s and 4.0 Hz. For this case the observed frequency (videotaped) of the slugs does not correspond to the perturbation frequency.

Table 5 shows the comparison between the propagation speed of void fraction waves as obtained from the voidmeters and the propagation speed of gas slugs as obtained from videotapes. Generally both speeds are consistent, indicating that in slug flow the propagating "structure" is the gas slug itself. In addition, the obtained speeds of propagation of the slugs are consistent with previous results (Tournaire 1987; Fréchou 1986).

4. BUBBLY–SLUG FLOW TRANSITION

The transition from bubbly to slug flow regimes has received significant attention over the years. Several analytical and empirical models have appeared with relative success. It is not the purpose

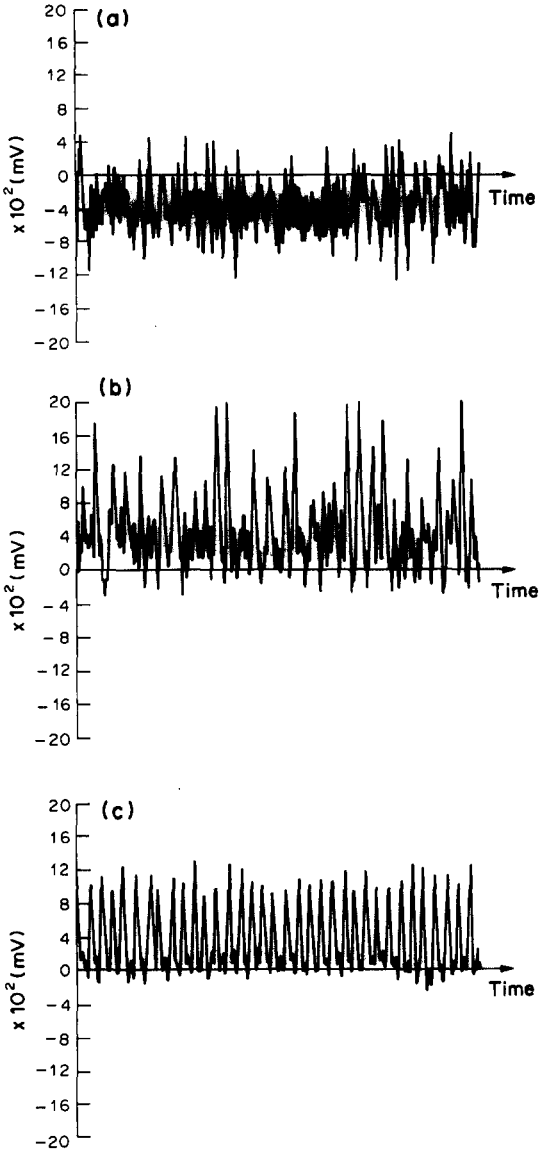

Figure 8. Signals from sensors for (a) bubbly, (b) transitional and (c) slug flow regimes.

of the present work either to readdress the problem from an analytical point of view or to establish a definitive empirical criterion. However, given the amount of experimental evidence gathered during the course of the present research, it is believed that some contribution to the transition problem can be made via a careful examination of the data.

The problem of the appearance of a second propagation speed has been discussed in previous sections. The second speed was related to the formation of an enlarged bubble structure which propagates with a speed higher than the average velocity of the gas. The appearance of this structure could be associated with the onset of the flow regime transition, since its characteristics are very similar to those presented by the slug flow regime. Among these characteristics, the propagation speed and the spectrum of signals from voidmeters can be included. Thus, a practical transition criterion could be proposed, according to which the onset of the slug flow regime would be attained at a given location when a "structure" appears, such that its propagation speed is higher than the average velocity of the gas phase, i.e.

$$C_2 > V_G, \qquad [1]$$

where C_2 is the second propagation speed and V_G is the average gas velocity. The proposed criterion does not require a subjective decision to be made, and does not require either complex

Table 4. Frequency of the slugs compared to that of the imposed perturbations

	$J_L = 0.275$ m/s			$J_L = 0.260$ m/s	
ϵ[a]	Imposed freq. (Hz)	Slug freq. (Hz)	ϵ[b]	Imposed freq. (Hz)	Slug freq. (Hz)
0.35	3.2	3.3	0.296	3.2	3.1
0.35	3.6	3.7	0.296	2.8	2.7
0.398	0 (NP)	3.4	0.296	1.1 & 2.2	2.1
0.398	2.5	2.5			
0.398	3.0	3.0			
0.398	4.0	2.6 (top TS) 3.5 (bottom)			

[a]$\epsilon = 0.35$ corresponds to $J_G = 0.198$ m/s; $\epsilon = 0.398$ corresponds to $J_G = 0.239$ m/s. [b]$\epsilon = 0.296$ corresponds to $J_G = 0.154$ m/s.

instrumentation, since only two impedance (or other) sensors are necessary. Further research is needed to validate the proposed transition criterion, but the present results seem to be encouraging. Table 6 illustrates the validity of the above criterion. The table shows the propagation speeds of naturally occurring void fraction waves; the operating conditions are given in the table. Note that for the case $J_L = 0.120$ m/s, the flow is bubbly up to measuring station 4. From that point on, transition occurs. The table displays only one propagation speed, which is the one corresponding to the dominant peak in the cross-correlation diagram. Figure 9(a) displays the cross-correlation diagram of signals from voidmeters located at the middle of the TS; two peaks, corresponding to the competing propagating structures, can be observed. For the other case listed in table 6, the slug flow regime occurs throughout the TS, since $C_2 > V_G$. The corresponding cross-correlation diagram is shown in figure 9(b); a single peak is observed.

Figure 9(a) illustrates the fact that the onset of the transition from the bubbly to slug flow regime can be determined through [1], under the condition of a two-peak cross-correlation between signals from the intervening voidmeters. If the criterion given by [1] is satisfied along with a one-peak cross-correlation, slug flow may occur if the void fraction is higher than that prior to the onset of the transition.

5. CONCLUSIONS

The literature on void fraction waves has been extended by a series of works in the last decade—works which have covered an extensive range of operating conditions and several

Table 5. Propagation speed as compared to the displacement speed of slugs

	$J_L = 0.275$ m/s			$J_L = 0.260$ m/s	
ϵ[a] f(Hz)	Propag. speed (m/s)	Slug speed (m/s)	ϵ[b] f(Hz)	Propag. speed (m/s)	Slug speed (m/s)
0.35 2.7	0.79	0.81	**0.397** 3.2	0.76	0.74
0.35 3.2	0.79	0.77	**0.296** 3.2	0.61	0.85
0.35 3.6	0.76	0.78	**0.296** 3.2	0.68	0.77
0.398 2.5	0.85	0.75			
0.398 3.0	0.85	0.79			
0.270 0.2 0.4 0.6	0.62	0.71			
0.296 0.3 0.5 1	0.71	0.72			

[a]$\epsilon = 0.35$ corresponds to $J_G = 0.198$ m/s; $\epsilon = 0.398$ corresponds to $J_G = 0.239$ m/s; $\epsilon = 0.270$ corresponds to $J_G = 0.135$ m/s; $\epsilon = 0.296$ corresponds to $J_G = 0.157$ m/s.
[b]$\epsilon = 0.397$ corresponds to $J_G = 0.243$ m/s; $\epsilon = 0.296$ corresponds to $J_G = 0.154$ m/s.

Table 6. Void propagation speeds along the TS (m/s)

Couple	$J_L = 0.120$ m/s $\epsilon = 0.388$ $V_G = 0.41$ m/s ($J_G = 0.159$ m/s)	$J_L = 0.260$ m/s $\epsilon = 0.40$ $V_G = 0.60$ m/s ($J_G = 0.243$ m/s)
1–2	0.32	
2–3	0.32	0.73
3–4	0.49	0.73
4–5	0.49	0.73
5–6	0.49	0.76
6–7	0.50	0.76
7–8	0.51	0.76
8–9	0.51	0.76

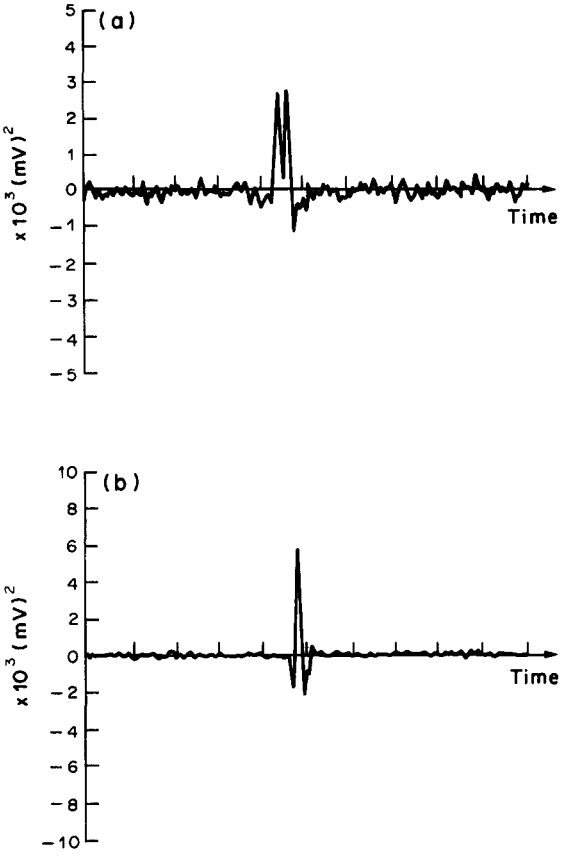

Figure 9. Cross-correlation diagrams: (a) transitional conditions, with two propagating structures—$J_L = 0.120$ m/s, $J_G = 0.159$ m/s, $\epsilon = 0.388$; (b) developed slug flow—$J_L = 0.260$ m/s; $J_G = 0.243$ m/s, $\epsilon = 0.40$. Natural perturbations.

configurations of two-phase gas–liquid flow. The purpose of the present work was to fill in some of the gaps left by previous research, aiming at the development of a topological law for the void fraction. However, and although further research is desirable, some interesting features of the problem have been elucidated:

—the attenuation phenomenon and its relation with coherence functions from adjacent sensors;
—the establishment of a transition criterion from the bubbly to slug flow regimes, based on the speed of propagation of void fraction waves;
—the relation between the motion of gas slugs and the void fraction propagation speed at relatively high void fractions, obtained both by signal processing and high-speed videotapes.

Acknowledgements—The first author gratefully acknowledges the support by the Fundacão de Amparo à Pesquisa do Estado de São Paulo, Brasil, and the Centre d'Etudes Nucléaires de Grenoble, France.

REFERENCES

BERNIER, R. J. M. 1982 Unsteady two-phases flow instrumentation and measurement. Ph.D. Thesis, California Inst. of Technology, Pasadena.

BOURÉ, J. A. 1988 Properties of kinematic waves in two-phase pipe flows; consequences on the modeling strategy. Presented at *European Two-phase Flow Group Mtg*, Brussels.

DELHAYE, J. M., FAVREAU, C., SAIZ-JABARDO, J. M. & TOURNAIRE, A. 1987 Experimental investigation on the performance of impedance sensors of two and six electrodes for area averaged void fraction measurements. Presented at *24th National Heat Transfer Conf.* Pittsburgh, Pa.

FRANÇA, F. A. 1987 Bubbly–slug and slug–churn transitions in a vertical adiabatic two-phase flow. Ph.D. Thesis. Univ. of Campinas, São Paulo, Brazil.

FRÉCHOU, D. 1986 Etude expérimentale de l'écoulment gas–liquide ascendant à deux et trois fluides en conduite verticale. *Revue Inst. Fr. Pétrole* **41,** 115.

JONES, O. C. & ZUBER, N. 1975 The interrelation between void fraction fluctuation and flow patterns in two-phase flow. *Int. J. Multiphase Flow* **2,** 273–306.

KYTÖMAA, H. K. 1986 Stability of the structure in multicomponent flows. Ph.D. Thesis, California Inst. of Technology, Pasadena.

MATUSZKIEWICZ, A., FLAMAND, J. C. & BOURÉ, J. A. 1987 The bubble–slug flow pattern transition and instabilities of void fraction waves. *Int. J. Multiphase Flow* **13,** 199–217.

MERCADIER, Y. 1981 Contribution à l'étude des propagations de perturbations de taux de vide dans les écoulements diphasiques eau–air à bulles. Thesis, Univ. Scientifique et Médicale et Inst. National Polytechnique de Grenoble, France.

MICAELLI, J. C. 1982 Propagation d'ondes dans les écoulements diphasiques à bulles à deux constituants. Thesis, Univ. Scientifique et Médicale et Inst. National Polytechnique de Grenoble, France.

PAUCHON, C. & BANERJEE, S. 1986 Interphase momentum interaction effects in the averaged multifield model. Part I: void propagation in bubbly flows. *Int. J. Multiphase Flow* **12,** 559–573.

SAIZ-JABARDO, J. M. 1987 Experiments on void fraction waves. Centre d'Etudes Nucléaires de Grenoble, Report SETh/LEF/87-1.

TOURNAIRE, A. 1987 Détection et étude des ondes de taux de vide en écoulement diphasique à bulles jusqu'à la transition bulles–bouchon. Thesis, Univ. Scientifique et Médicale et Inst. National Polytechnique de Grenoble, France.

WALLIS, G. B. 1969 *One-dimensional Two-phase Flow*. McGraw-Hill, New York.

ZUBER, N. & FINDLAY, J. 1965 Average volumetric concentration in two-phase flow systems. *Trans. ASME Jl Heat Transfer* **87,** 453.

ZUBER, N. & HENCH, J. 1962 Steady state and transient void fraction of bubbling systems and their operating limits. Part II: transient response. General Electric Report 62GL111.